JOURNAL OF CATALYSIS 144, 30–37 (1993)

Pt–Au/Al_2O_3 Catalysts: Preparation, Characterization, and Dehydrogenation Activity

D. ROUABAH AND J. FRAISSARD

Laboratoire de Chimie des Surfaces, associé au CNRS URA 1428, Université Pierre et Marie Curie, 4 Place Jussieu, 75252 Paris Cedex 05, France

Received August 6, 1992; revised June 17, 1993

The physicochemical characteristics of Pt–Au catalysts, such as the dispersion, chemisorption, and thermodesorption of hydrogen, have been studied in terms of gold content. The catalysts were prepared by coimpregnation of a γ-alumina by a mixture of hexachloroplatinic and tetrachloroauric acids, calcination in oxygen and slow reduction in H_2–He from 25 to 400°C. The most outstanding result is the very large increase in the dispersion with the gold concentration. For example, with the alloy containing 80% gold more than 70% of the detectable particles are below 10 Å. In the same way, the activity per site and the selectivity in the dehydrogenation of methylcyclohexane to toluene increase with the gold concentration. © 1993 Academic Press, Inc.

INTRODUCTION

Almost all the processes for transforming hydrocarbons require heterogeneous catalysis. Supported metals and sometimes metal complexes are commonly employed in this field. The metals are often noble metals such as Pt, Pd, and Rh. The use of bimetallic catalysts is in full expansion, particularly in petrochemistry and refining.

Hydrocarbon conversion reactions have been studied on Pt in the form of films, crystals, or supported metals; then the studies were extended to alloys such as Pt–Re (*1*), Pt–Ir (*2*), and Pt–Sn (*3, 4*) in order to study the effect of the second metal on the hydrogenating and dehydrogenating properties of the Pt. The addition of gold to Pt arouses much curiosity, this metal being considered as an inactive element when it is used alone in catalysis. Nevertheless, some authors think that, combined with another metal, gold can play a role more important than that of a diluent for the metal presumed to be active.

There has already been work on these bimetals: Pt–Au films (*5–10*), mono- and polycrystals (*11–13*), and supported Pt–Au alloys (*14–19*). It has been observed (*16*) that in certain catalytic processes, such as the conversion of *n*-hexane to methylcyclopentane, the activity of alloys is much higher than that of pure Pt.

In this paper the physicochemical characteristics of Pt–Au catalysts, such as the dispersion, chemisorption, and thermodesorption of hydrogen, have been studied in terms of the gold content. The dehydrogenation of methylcyclohexane has been used as a test of the catalytic activity.

EXPERIMENTAL CONDITIONS

Catalyst Preparation

The catalysts were prepared by coimpregnation of γ-aluminium oxid C from Degussa, (100 ± 15 m^2/g) with a mixture of hexachloroplatinic and tetrachloroauric acids in known proportions. The mixture is heated to 90°C with continuous stirring. After drying, the sample is then calcined in oxygen flow for 1 h at a temperature T_c of 400°C (heating rate = 1°C/min). After cooling in helium, the metal is reduced in He–H_2 at temperature T_r = 400°C for 12 or 120 h (same heating rate from 25°C to T_r°C). The total mean concentration is 10% w/w. The cata-

0021-9517/93 $5.00
Copyright © 1993 by Academic Press, Inc.
All rights of reproduction in any form reserved.

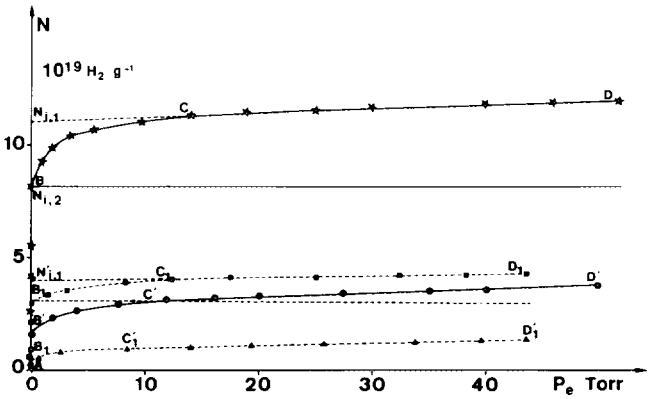

FIG. 1. Hydrogen adsorption isotherms for samples Pt_{100} and Pt_{20}: full line, Pt_{100}; dotted line, Pt_{20}. ABCD or $AB_1C_1D_1$, total adsorption; AB'C'D' or $AB'_1C'_1D'_1$, physical adsorption.

lysts are denoted Pt_x, where x indicates the weight fraction of Pt ([Au] = (100 − x)%). This was determined by elemental analysis after reduction to the metals.

Dispersion, Catalytic Activity, and Temperature-Programmed Desorption

The dispersion, D, is mainly determined by transmission electron microscopy (Jeol 100 CX II). H_2 chemisorption is performed on a volumetric apparatus thermostated at 26.5°C.

The dehydrogenation of methylcyclohexane is carried out in a dynamic fixed bed reactor fitted with a glass frit on which 500 mg of catalyst are placed. The setup is placed in an oven whose temperature is controlled by a programmer. The reactant is circulated through the catalyst by means of a pump with a glass piston at a flow rate of 17.68 ml/h. The reaction occurs at a total pressure close to atmospheric pressure, without hydrogen or carrier gas. Samples are taken at regular time and temperature intervals. The reactor effluent is analysed on an Intersmat IGC 12M fitted with a catharometer and a 2-m Squalane column. Under the most severe experimental conditions, the degree of conversion with the most active catalyst was less than 50%.

In the TPD experiments 300 mg of catalyst are used and the effluent hydrogen is detected after going through a 1-m Porapaq Q G. C. column.

EXPERIMENTAL RESULTS

Hydrogen Chemisorption

The H_2 adsorption isotherms at 26.5°C are the same classical shape for all samples (except Pt_0), that is, with two regions AB and CD (Fig. 1). The first indicates strong H_2 chemisorption; the second corresponds both to saturation of the monolayer of the metal surface and to H_2 physisorption. There are theoretically two ways, [a] and [b], of determining the amount of H_2 chemisorbed at the monolayer.

[a] One extrapolates the intersection of the variation CD of the total adsorbed H_2, N_T, to zero pressure ($N_{i,1}$). $N_{i,1}$ corresponds to the monolayer.

[b] After saturation the sample is desorbed at 26.5°C and 10^{-5} Torr (1 Torr = 133.3 N m^{-2}) for a few minutes to eliminate the physisorbed H_2. To determine the latter, N_{phys}, H_2 is then readsorbed under the same conditions. In this case the amount of H_2 chemisorbed at the monolayer ($N_{i,2}$) is given by the difference between the isotherms ABCD and AB'C'D'.

Table 1 shows that the amounts $N_{i,1}$ and $N_{i,2}$ decrease almost monotonically with the Pt concentration. When one goes from Pt_{100}

TABLE 1

The Amounts of H_2 Chemisorbed $N_{i,1}$ and $N_{i,2}$

Sample	T_c and T_r (°C)	$N_{i,1}$ (H_2 g^{-1})	$N_{i,2}$ (H_2 g^{-1})
Pt_{100}	400	11.1×10^{19}	8.2×10^{19}
Pt_{95}	400	10.7×10^{19}	8.2×10^{19}
Pt_{80}	400	8.2×10^{19}	6.0×10^{19}
Pt_{60}	400	7.2×10^{19}	5.7×10^{19}
Pt_{50}	400	7.6×10^{19}	6.1×10^{19}
Pt_{40}	400	4.3×10^{19}	3.2×10^{19}
Pt_{20}	400	4.0×10^{19}	3.1×10^{19}

to Pt_{20} the Pt concentration and the values of N_i decrease by a factor of 5 and 2.5, respectively. Compared to the same amount of Pt there is therefore twice as much as H_2 chemisorbed on the Pt_{20} alloy than on pure Pt.

The dispersions of Pt_{100} deduced from $N_{i,1}$ and $N_{i,2}$ are $D_1 = 0.72$ and $D_2 = 0.55$, respectively. The mean particle diameters calculated from the $D = f(d_m)$ curve (*20*) are 16 and 23 Å, respectively.

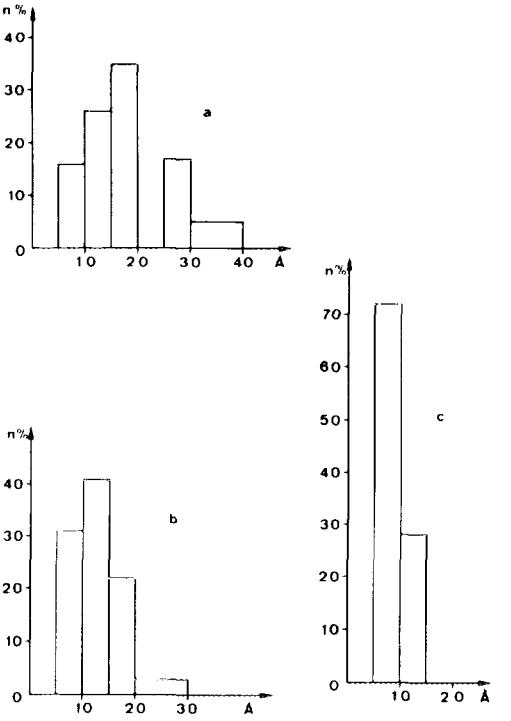

FIG. 2. Histograms of samples (a) Pt_{100}, (b) Pt_{50}, and (c) Pt_{20}.

Electron Microscopy

Electron microscopy is theoretically the most direct method for determining the dispersion since it is usually possible to see the particles and to measure their size. The photographs of the samples in most cases reveal a relatively homogeneous distribution of metal particles; we have also calculated the mean particle diameter, d_m, by the equation $d_m = \Sigma n_i d_i / \Sigma n_i$, where n_i is the number of particles of diameter d_i. It is found that the metal dispersion determined by EM increases with the gold concentration (Table 2 and histogram, Fig. 2).

The dispersion is already good for Pt_{100}

TABLE 2

Catalyst Particle Size Distribution

Sample	T_r (°C)	% of particles of diameter d (Å)						d_m
		<10	10–15	15–20	20–25	25–30	30–40	
Pt_{100}	400	16	26	35	0	17	5	20
Pt_{95}	400	24	44	27	3	2	0	14
Pt_{80}	400	40	26	24	2	5	3	15
Pt_{60}	400	33	36	23	0	6	2	14
Pt_{50}	400	31	41	22	3	3	0	14
Pt_{40}	400	28	48	20	4	0	0	15
Pt_{20}	400	72	28	0	0	0	0	<10

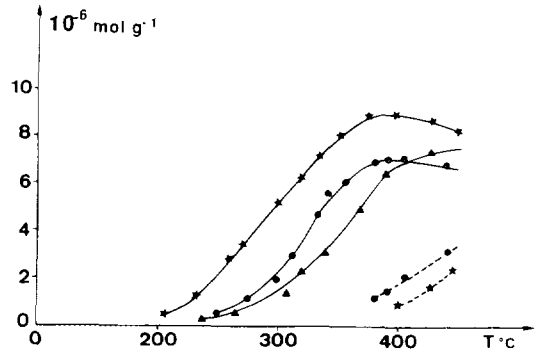

FIG. 3. Variation of the number of moles of toluene and benzene with the temperature: ●, Pt_{100}; ★, Pt_{50}; ▲, Pt_{20}; full line, toluene; dotted line, benzene.

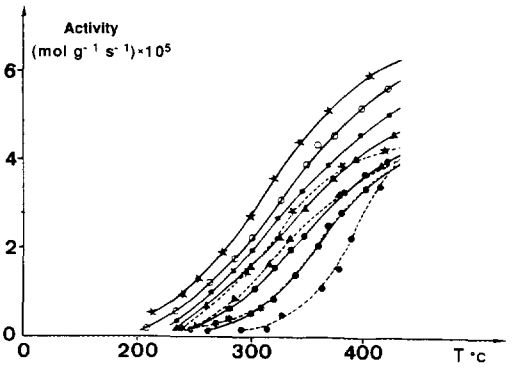

FIG. 4. Temperature dependence of the catalytic activity per gram of series A and B: dotted line, series A; full line, series B; ⊛, Pt_{100}; ▲, Pt_{80}; ○, Pt_{60}; ★, Pt_{50}; ■, Pt_{40}; ●, Pt_{20}.

since 77% of the particles are below 20 Å in diameter. It is excellent with Pt_{20} (100% of the particles below 15 Å).

Catalytic Activity

Methylcyclohexane was catalytically converted in the temperature range 150°C < T_e < 500°C. The reaction is mainly dehydrogenation. Nevertheless, more or less large amounts of benzene can be detected when $T_e \geq 400$°C. To determine the most appropriate experimental conditions we did preliminary trials on certain samples using 1 g of catalyst and a flow rate of 1.768 ml/h. The reaction is detectable as of $T_e = 230$°C under these experimental conditions. The amount of benzene which appears at high temperature ($T_e \geq 400$°C) decreases when the Au concentration is high (Fig. 3). It decreases significantly from Pt_{100} to Pt_{50} and is negligible for Pt_{20}. In order to avoid this cracking reaction we have therefore decreased the contact time by increasing the flow rate (17.65 ml) and by halving the sample weight. Figure 4 shows the variation of the catalytic activity per gramme of solid with the temperature T_e for four samples reduced at 400°C for 12 h (series A).

For T_e < 400°C we note that Pt_{100} is less active than the alloys Pt_{80} and Pt_{50}. Pt_{20} is the least active of the series. For $T_e \geq 400$°C the activity differences decrease, but in the high-temperature zone phenomena such as diffusion can be involved.

The results obtained for the samples of series B, for which the reduction time has been extended to 120 h, are significantly different. The activity of Pt_{100}-series B is identical to that of Pt_{100}-series A, but those of the alloys are very much increased (Fig. 4) and that of Pt_{20} becomes greater even than that of Pt_{100}.

As an example, Fig. 5 gives for $T_e = 350$°C the variation of the activity per gram for the two series. In both cases this activity goes through a maximum for Pt_{50}. The catalytic activity per gram therefore depends on gold content and, for alloys, on the reduction time.

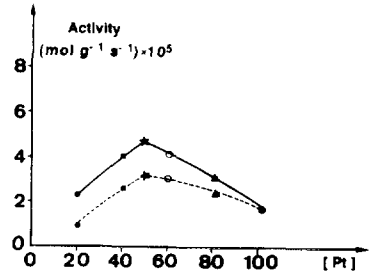

FIG. 5. Dependence of the activity per gram on the gold concentration for $T_e = 350$°C: dotted line, series A; full line, series B.

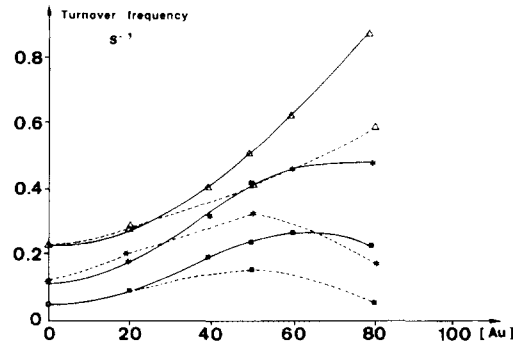

FIG. 6. Dependence of the activity per active site on the gold concentration for series A and B: dotted line: series A; *full line*, series B; ■, 300°C; ★, 350°C; △, 400°C.

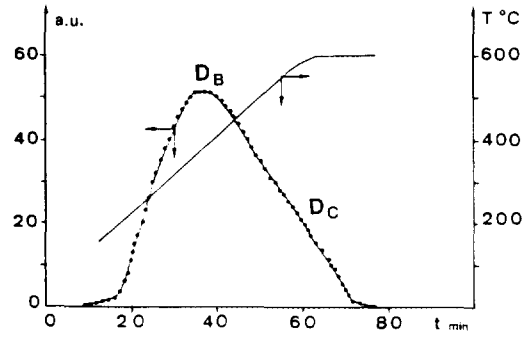

FIG. 7. Temperature-programmed desorption profile of sample Pt_{100}. a.u., arbitrary units; t, time in minutes.

The results are even clearer when the activity per active site is plotted against the gold concentration (Fig. 6). The numbers of active sites considered are equivalent to the numbers of H atoms chemisorbed at the monolayer, determined under the same conditions as for the measurement of the Pt dispersion alone without making any assumption about the nature of the site, Pt or Au. For the two series at T_e = 300 or 350°C the activity per site increases with the gold concentration, goes through a maximum when this is close to 50–60%, then decreases or becomes almost constant (series B, 350°C). For T_e = 400°C, on the other hand, this variation is monotonic when one goes from Pt_{100} to Pt_{20}; the activity per site is multiplied by a factor of 2.5 or 4 for series A and B, respectively.

Temperature-Programmed Desorption (TPD)

TPD is frequently used to study metal catalysts. The principle of this technique consists in sweeping the sample with an inert gas and analysing the chemical species desorbed when the temperature is increased rapidly. The TPD profile of the Pt_{100} sample (Fig. 7) consists of a single asymmetric signal with a maximum D_B of hydrogen desorption at 400°C and a shoulder D_c at about 590°C. The intensity of the former represents 83% of the total desorption, and that of the second 17%. These two signals are much better resolved on the profiles of Pt_x catalysts (Fig. 8). Moreover, an important third signal D_A is observed at 260°C. If after the first thermodesorption we perform another cycle which consists of a new reduction followed by thermodesorption (Fig. 9) the three previous signals are found again, but peak D_B is very weak. Species A, corresponding to D_A, predominates.

If the reduction time is extended to 1 month, peak D_A is replaced by two others, $D_{A'}$ and $D_{A''}$, for which the maximum temperatures of hydrogen desorption are around 200 and 300°C, respectively (Fig. 10).

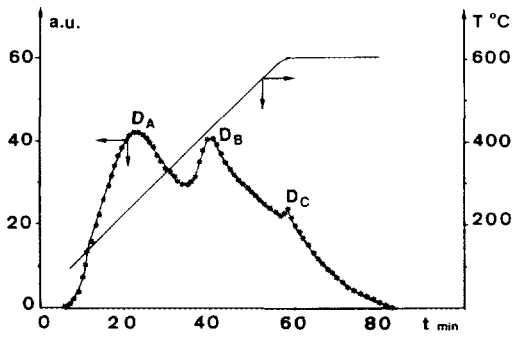

FIG. 8. Temperature-programmed desorption profile of sample Pt_{50} (first reduction–desorption cycle). a.u., arbitrary units; t, time in minutes.

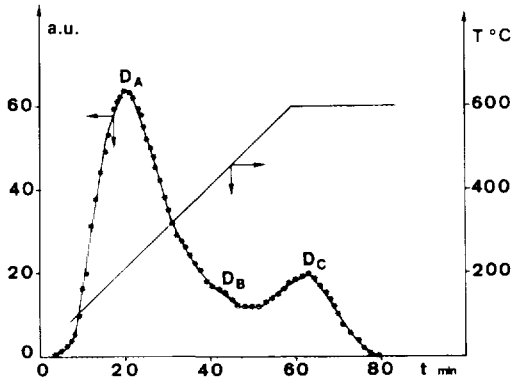

FIG. 9. Temperature-programmed desorption profile of sample Pt_{50} (second reduction–desorption cycle). a.u., arbitrary units; t, time in minutes.

DISCUSSION AND CONCLUSION

Let us first consider the dispersion of sample Pt_{100}. As for the amounts of chemisorbed H_2 (Table 1) we observe firstly that $N_{i,1}$ is greater than $N_{i,2}$. The difference is 20%, therefore not negligible. The dispersions deduced from these two numbers are 0.72 and 0.55, respectively. The corresponding average sizes calculated from the curve of D against d_m (*20*) are 16 and 23 Å, respectively. Comparison with EM results seems to prove that the value $N_{i,2}$ of the number of H_2 molecules adsorbed at the monolayer is the more plausible.

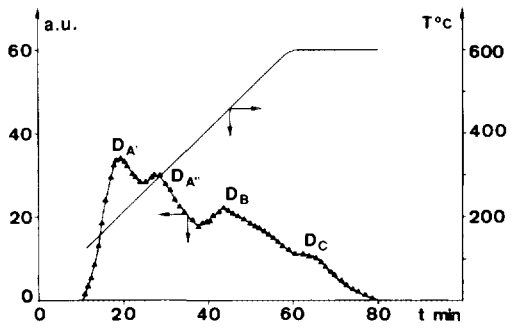

FIG. 10. Temperature-programmed desorption profile of sample Pt_{20} (reduction time, 1 month). a.u., arbitrary units; t, time in minutes.

In reality the true value of N_i must lie between $N_{i,1}$ and $N_{i,2}$. $N_{i,1}$ must be an overestimate because of the presence of physisorbed H_2 and spillover H_2 which exists when θ is greater than about 0.5. $N_{i,2}$ is an underestimate since by pumping at 25°C the hydrogen weakly chemisorbed at about θ = 1 must be desorbed at the same time as the physisorbed species. Moreover, it is possible that the very small particles are not detected by EM. There must, however, be very few since they were not detected by ^{1}H-NMR of chemisorbed hydrogen (*21*). The chemical shift of chemisorbed H_2 depends on the particle size (*22, 23*).

Table 2, which presents the EM data, shows that the addition of gold contributes markedly to the formation of very small particles leading to excellent dispersions. The mean particle diameters of samples with a high gold concentration do not exceed 15 Å, whereas for a sample of pure Pt it has a value of about 20 Å. For Pt_{20}, 72% of the particles which can be detected are below 10 Å. This result may seem surprising, in view of the difficulty of preparing very small particles of pure gold by reduction above 200°C. Perhaps our preparation is responsible for this dispersion. Indeed if one reduces gold and platinum in H_2 alone, directly at 400°C, *large particles are obtained;* if, on the other hand, the system is swept with the H_2–He mixture (total pressure about 1 atm, $P_{H_2} \sim P_{He}$) right from 25°C with a very slow temperature increase up to 400°C (1°/min), the dispersion mentioned is obtained.

One also observes that the number of chemisorbed H_2 molecules per gramme of sample Pt_x decreases with the Pt concentration, but by a factor of 2.5 when the latter varies by a factor of 5. This indicates that the number of H_2 adsorbed per atom of Pt increases with [Au]. The amounts defined in this way make no assumption about the nature of the sites where the H_2 is chemisorbed (Pt or Au); however, this can be explained a priori by

—increase of the concentration of spillover H_2;

—preferential location of the Pt at the surface of the particles associated with a greater dispersion. In particular, if there are very small Pt islets on the surface these can chemisorb more than one hydrogen atom per surface Pt atom. It is well known that the stoichiometry of H/Pt chemisorption is greater than unity for very small particles of Pt located in the channels or cavities of zeolite supports.

—adsorption on gold of H_2 previously dissociated on Pt.

In view of the results obtained by temperature-programmed desorption (TPD), the third hypothesis seems the most plausible. TPD of sample Pt_{100} shows that there are two signals D_B and D_C corresponding to two different species, B and C (Fig. 7). Signal D_B, which has a maximum at 400°C, must be attributed to H_2 chemisorbed on Pt atoms, in agreement with results obtained by other authors for Pt supported (*24*) or not (*25, 26*). The shoulder D_C at about 590°C is attributed to the support, i.e., to spillover H_2 (*14, 24*). This species represents 17% of the total desorbed from sample Pt_{100}. When gold is added, the two first signals still exist but they are better resolved. However, the small variation of the intensity of D_C with the Au concentration excludes the first hypothesis. This is quite reasonable, since the spillover depends above all on the surface properties of the support which is the same for all the samples. A third signal D_A is detected at 260°C and its intensity increases with the gold concentration and the reduction time at the expense of D_B (Fig. 9). After long treatment, at high temperature, the intensity of D_B is nearly zero. Signal D_A therefore can only correspond to H_2 chemisorbed either on the Pt–Au alloy particles or on the very small Pt islets separated by gold; the lower the Pt concentration the more islets there will be. The position proves that the interaction of H_2 with the alloy or with the very small islets is weaker than in the case for Pt_{100}. We think, however, that if the second hypothesis were valid, the intensity of peak D_B should not go to zero equally well for 80% Pt as for 50%. For this reason we propose the third hypothesis.

This result can explain the increase in catalytic activity with the gold concentration. The species obtained by dehydrogenation on Pt migrate onto the gold where they are more easily desorbed, which in this way facilitates chemisorption of the reactants. If this is the case the rate-determining step for dehydrogenation on Pt would be the desorption of the reaction products.

The variation of the activity per gramme of solid with the gold concentration (Fig. 4), in particular, the existence of a maximum at about 50% (Fig. 5), confirms that the activity of Pt_x catalysts cannot be due to an additive effect of particles of pure Pt and Au, but to a synergetic effect due to the creation of alloy particles. A similar phenomenon of increased activity has been observed by other authors (*10*) for Pt–Au/SiO_2 alloys. Except for sample Pt_{100}, the activities per gram (Fig. 4) or per site (Fig. 6) of samples B are greater than those of the A homologues. The activity increases therefore with the reduction time, at least between 12 and 120 h. This variation, especially marked when the gold concentration is high, could be related to the time required for the formation of the alloy from the Pt and Au metal particles. The Pt_{20} sample reduced for 1 month shows two species of H_2 desorbed from the alloy, corresponding probably to two types of alloy particles distinguished by their Pt/Au ratio and their metal distribution at the surface. However, it would be unwise to try to associate these two compositions with those defined by the well known phase diagram for bulk Pt–Au.

REFERENCES

1. Kluksdahl, H. E., U.S. Patent **3,** 415, 737 (1968).
2. Sinfelt, J. H., U.S. Patent **3,** 953, 368 (1976).
3. Dantzenberg, F. M., German Offenlegungs-schuft. **2,** 12, 765 (1971).
4. Rausch, R. E., U.S. Patent **3,** 632, 525 (1972); U.S. Patent **3,** 745, 112 (1973).
5. Clarke, J. K. A., Kane, A. F., and Baird, T., *J. Catal.* **64,** 200 (1980).

6. Alan, F., and Clarke, J. K., *J. Chem. Soc. Faraday Trans.* **76,** 1640 (1980).
7. Stephan, J. J., and Ponec, V., *J. Catal.* **42,** 1 (1976).
8. Kuijers, F. J., Dessing, R. P., and Sachtler, W. M. H., *J. Catal.* **33,** 316 (1974).
9. Stephan, J. J., Ponec, V., and Sachtler, W. M. H., *Surf. Sci.* **47,** 403 (1975).
10. Bouwman, R., and Sachtler, W. M. H., *J. Catal.* **19,** 127 (1970).
11. Sachtler, J. W. A., and Somorjai, G. A., *J. Catal.* **89,** 35 (1984).
12. Yeates, R. C., and Somorjai, G. A., *J. Catal.* **103,** 208 (1987).
13. Biloen, P., Bouwman, R., Van Santen, R. A., and Brongersma, H. H., *in* "Proceedings, 7th International Vacuum Congress, and 3rd International Conference on Solid Surfaces, 1977," Vol. 2, p. 1401.
14. Anderson, J. R., Foger, K., and Breakspere, R. J., *J. Catal.* **57,** 458 (1979).
15. Foger, K., and Anderson, J. R., *J. Catal.* **61,** 140 (1980).
16. Clarke, J. K. A., Manninger, L., and Baird, T., *J. Catal.* **54,** 230 (1978).
17. Van Schaik, J. R. H., Dessing, R. P., and Ponec, V., *J. Catal.* **38,** 273 (1975).
18. Galvagno, S., and Parravano, G., *J. Catal.* **57,** 272 (1979).
19. O'Cinneide, A., and Gault, F. G., *J. Catal.* **37,** 311 (1975).
20. Van Hardeveld, R., and Hartog, F., *Surf. Sci.* **15,** 189 (1969).
21. Rouabah, D., Benslama, R., and Fraissard, J., *Chem. Phys. Lett.* **179,** 218 (1991).
22. Reinecke, N., and Haul, R., *Ber. Bunsenges Phys. Chem.* **88,** 1232 (1984).
23. De Menorval, L. C., and Fraissard, J. P., *Chem. Phys. Lett.* **77,** 309 (1981).
24. Kramer, R., and Andre A., *J. Catal.* **58,** 287 (1979).
25. Peng, Y. K., and Dawson, P. T., *Can. J. Chem.* **53,** 298 (1975).
26. Stephan, J. J., Ponec, V., and Sachtler, W. M. H., *J. Catal.* **37,** 81 (1975).